Structural mechanism of DNA recognition by the p204 HIN domain

Xiaojiao Fan[1], Jiansheng Jiang[2], Dan Zhao[1], Feng Chen[1], Huan Ma[1], Patrick Smith[2], Leonie Unterholzner[3], Tsan Sam Xiao[4], and Tengchuan Jin*[1, 5]

[1]Hefei National Laboratory for Physical Sciences at Microscale, the CAS Key Laboratory of Innate Immunity and Chronic Disease, School of Basic Medical Sciences, Division of Life Sciences and Medicine, University of Science and Technology of China, Hefei, 230027 China

[2]Laboratory of Immune System Biology, National Institute of Allergy and Infectious Diseases, National Institutes of Health, Bethesda, MD 20892 USA

[3]Division of Biomedical and Life Sciences, Faculty of Health and Medicine, Lancaster University, Lancaster LA1 4YQ, UK

[4]Department of Pathology, Case Western Reserve University, Cleveland, OH 44106 USA

[5]CAS Center for Excellence in Molecular Cell Science, Shanghai, China

*To whom correspondence should be addressed. T.J., Tel: +86-551-63600720; Email: jint@ustc.edu.cn.

This file includes:

Supplementary Tables S1 to S5

Supplementary Figures S1 to S8

Table S1. SAXS data collection, structural parameters and model statistics.

	p204 HINab (TJ4)
Data-collection parameters	
Beamline/Instrument	X9 at NSLS-I
Wavelength (Å)	1.033
q range recorded (Å^{-1})	0.004–0.360
Exposure time (seconds)	1.0
Concentration range (mg/ml)	1.00–3.80
Temperature (K)	293
Structural parameters	
q range used (Å^{-1})	0.020–0.208
$I(0)$ (cm^{-1}) [from Guinier]	107.81 ± 2.12
R_g (Å) [from Guinier]	31.13 ± 0.91
s R_g limits	0.65–1.25
$I(0)$ (cm^{-1}) [from $P(r)$]	107.40
R_g (Å) [from $P(r)$]	31.54
D_{max} (Å)	97.00
Porod volume estimate (Å^3)	27,816
Molecular-mass determination	
Molecular Mass Mr [from $I(0)$]	43,100
Molecular Mass [from PDB model]	44,916
Model results and validation	
NSD* (standard deviation)	0.633 (0.036)
No. runs [models for averaging]	10
Symmetry enforced	P1
χ^2 (q max) in fitting experimental data	0.192 (0.205)

* Normalized spatial discrepancy

Table S2. List of DNA oligonucleotides used in FP assay.

oligonucleotides	Sequence (5′–3′)
16 mer-S	CCATCAGAAAGAGAGC
16 mer-R	GCTCTCTTTCTGATGG
20 mer-S†	TAAGACACGATGCGATAAAA
20 mer-R†	TTTTATCGCATCGTGTCTTA
30 mer-S††	CCATCAGAAAGAGGTTTAATATTTTTGTGA
30 mer-R††	TCACAAAAATATTAAACCTCTTTCTGATGG

These DNA oligonucleotides were labeled with 5′-Fluorescein (FAM) at the sense (S) strand and annealed to its reverse (R) complement strand to form blunt-ended dsDNA.

†This oligo sequence was derived from the genomic sequence of human alphaherpesvirus.

††This oligo sequence was derived from the genomic sequence of vaccinia virus.

Table S3. RMSD values of the structural comparison of HIN domains.

RMSD (aligned numbers of Cα atom) Å	p204 HINa (PDB: 5YZP)	p204 HINb (PDB: 5YZW, molecule A)
p204 HINb (PDB: 5YZW, molecule A)	1.24 (180)	–
p204 HINb (PDB: 5YZW, molecule B)	1.25 (183)	0.60 (188)
IFI16 HINa (PDB: 2OQ0)	1.27 (187)	1.38 (183)
IFI16 HINb (PDB: 3B6Y)	1.37 (180)	1.15 (180)
p202 HINa (PDB: 4JBJ)	0.99 (183)	1.28 (179)
p202 HINb (PDB: 4L5T)	1.72 (166)	1.65 (173)

RMSD: root mean square deviation.

Table S4. Mutations of p204 HINab and HINa.

Mutants	Mutation sites at HINa domain	Mutation sites at HINb domain
HINab-m1	Y263A, K327A, D330A, K333A, F340A	–
HINab-m2	K279A, N316A, R320A, R415A	–
HINab-m3	–	R482A, N518A, R521-523A, K587A
HINab-m4	Y263A, K327A, D330A, K333A, F340A	R482A, N518A, R521-523A, K587A
HINab-m5	K279A, N316A, R320A, R415A	R482A, N518A, R521-523A, K587A
HINa-m1	Y263A, K327A, D330A ,K333A, F340A	–
HINa-m2	K279A, N316A, R320A, R415A	–

Table S5. Linkers of HIN domains in p204, p202, and IFI16.

Protein	Positions of HINa (HIN1)	Linker (residue)	Positions of HINb (HIN2)
p204	216–412	413–426 (SKRGNVPKEPAKEE)	427–619
p202	46–242	243–253 (EK---LLKESFEGD)	254–445
IFI16	192–393	394–514 (a loop/helix wrapper)	515–706

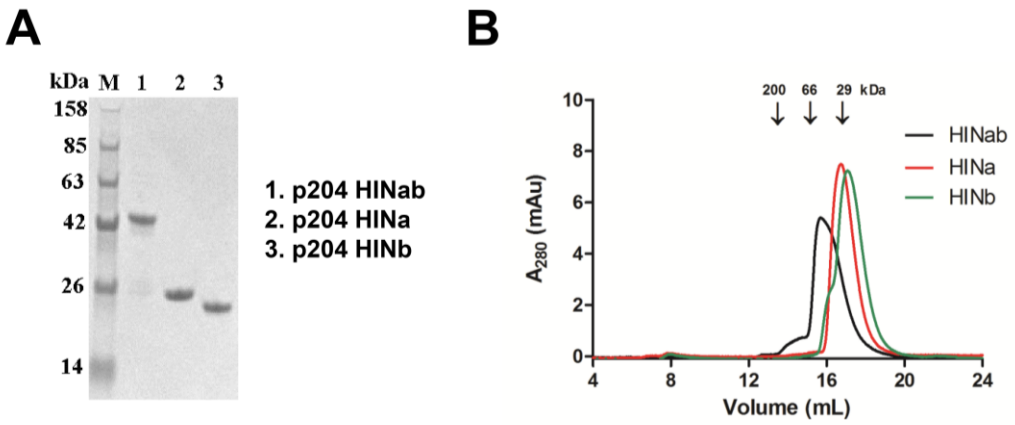

Figure S1. The purity and aggregation state of p204 HIN domains. (A) An SDS-PAGE image of purified p204 HINab, HINa, and HINb domains. (B) Size exclusion chromatography of purified p204 HINab, HINa, and HINb domains. All elution volumes correspond to monomers according to the marker (Sigma-Aldrich).

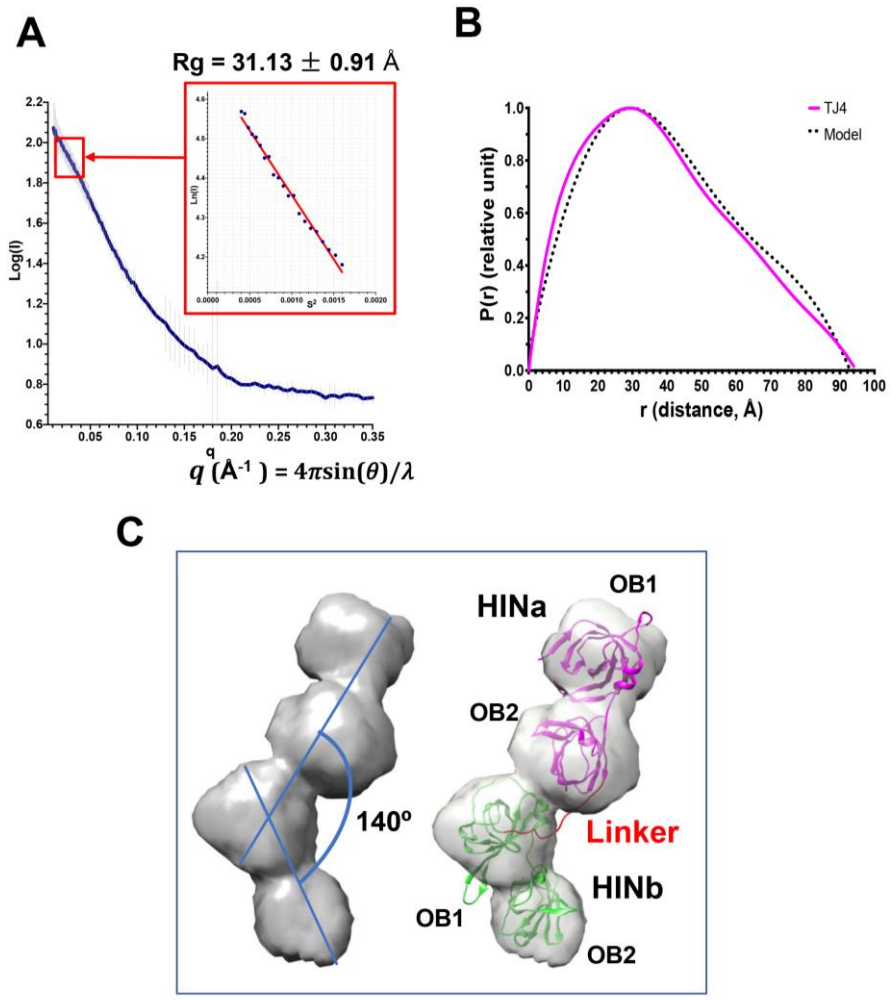

Figure S2. The SAXS data analysis of p204 HINab. (A) SAXS scattering intensity profile of p204 HINab. It is plotted as Log (I) against q [q (Å^{-1}) = $4\pi\sin(\theta)/\lambda$] shown in blue, the insertion figure is a Guinier plot that a linear fit (red line) produced Rg = 31.13 Å. (B) Pairwise distance distribution of p204 HINab. P(r) as a function of r for the experimental data (red curve) and for a coordinate model that fitted on the SAXS envelope (black dotted curve). (C) The molecular envelope of p204 HINab. *Ab initio* modelling (DAMMIF) was used to generate 20 shape reconstructions from the data, a molecular envelope of p204 HINab is shown in gray, revealing a cluster of four domains of OB. The dimensions of the envelope are 103.5Å x 54.0Å x 44.5Å. On the right, p204 HINab model is fitted into the SAXS envelope. It shows HINa at the top of two OB domains, HINb at the down of two OB domains, a hinge angle between HINa (pink) and HINb (green) measures about 140° (on the left figure).

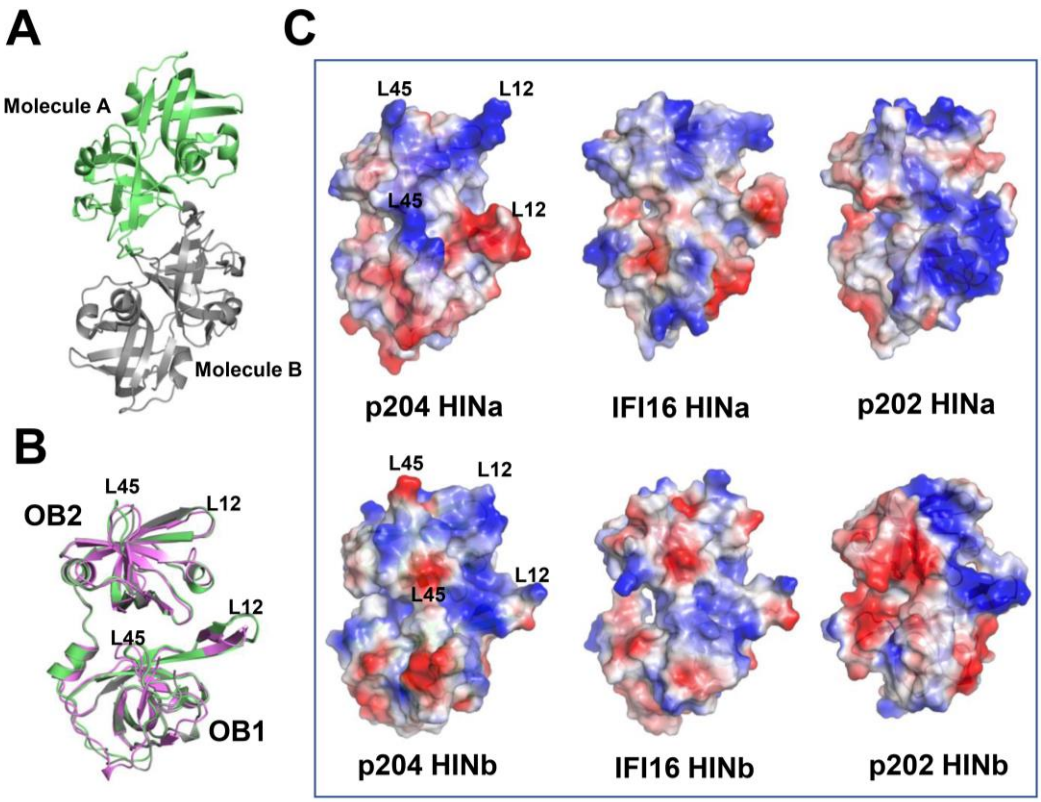

Figure S3. Structural comparisons of HIN domains in PYHIN family. (A) Structures of two p204 HINb molecules in the asymmetric unit. Molecule A is shown in lime and molecule B is shown in gray. (B) Structural superposition of p204 HINa and HINb. HINa is shown in violet. Two HINb molecules are shown in lime and gray, respectively. (C) Surface electrostatics of HIN domains in p204, IFI16 and p202. The electrostatic potential is shown in blue (positive charges) and red (negative charges). They were set to 20% transparency.

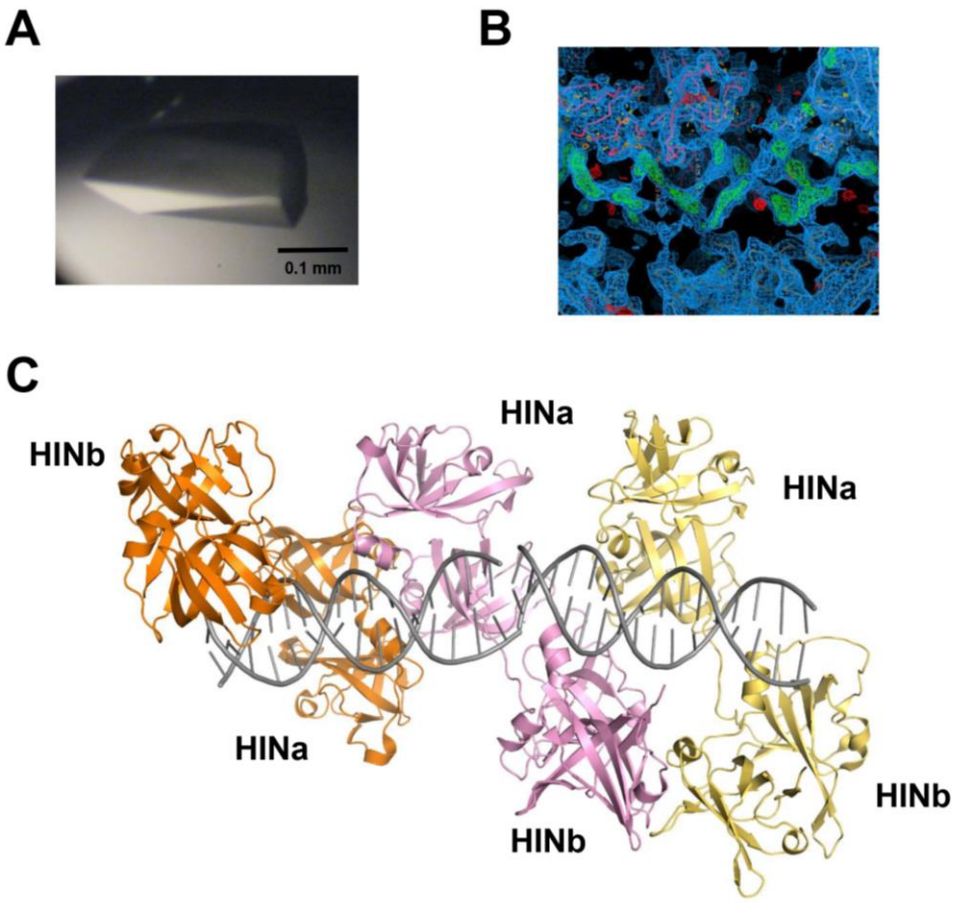

Figure S4. Crystal and structure of p204 HINab: DNA complex. (A) Crystal of p204 HINab: DNA complex. (B) The electron density map (Fo-Fc) of dsDNA bound to p204 HINab, contoured at 2.0 σ. (C) Structural model of p204 HINab:dsDNA complex in the asymmetric unit. Three p204 HINab molecules are shown in orange, pink, and yellow orange, respectively. Two copies of dsDNA are shown in gray.

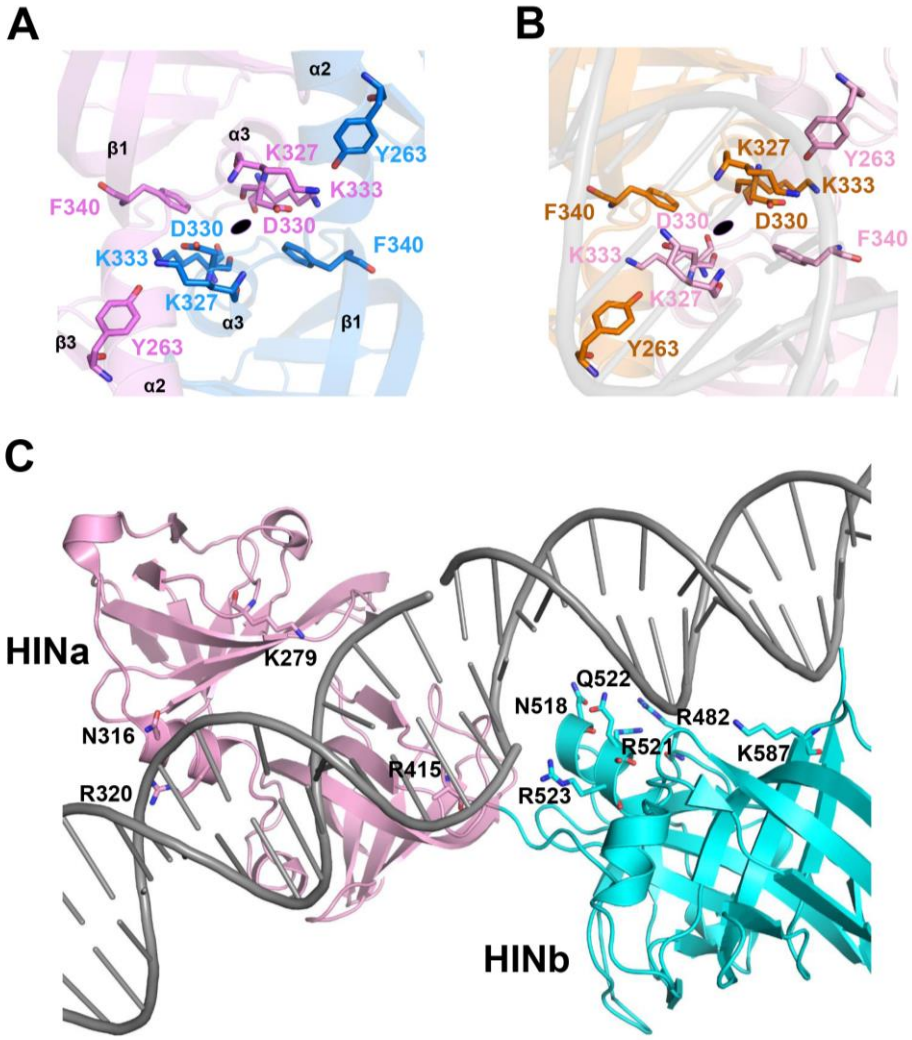

Figure S5. Interaction interface of p204 HINa dimer and HINab:dsDNA complex. (A) and (B) Dimeric interface of HINa in structures of p204 HINa and HINab:dsDNA complex. HINa dimer from p204 HINa structure is shown in violet and slate. HINa dimer from p204 HINab:dsDNA complex is shown in orange and pink. Residues involved in the dimerization are shown in sticks and labeled with the same colour as their structures. HINa and dsDNA were set to 80% transparency. Residues are below dsDNA in the actual HINab:dsDNA complex structure. (C) Interaction interface between p204 HINab and dsDNA. HINa is shown in pink and HINb is shown in cyan in p204:dsDNA complex structure. Interface residues are shown in sticks and labeled.

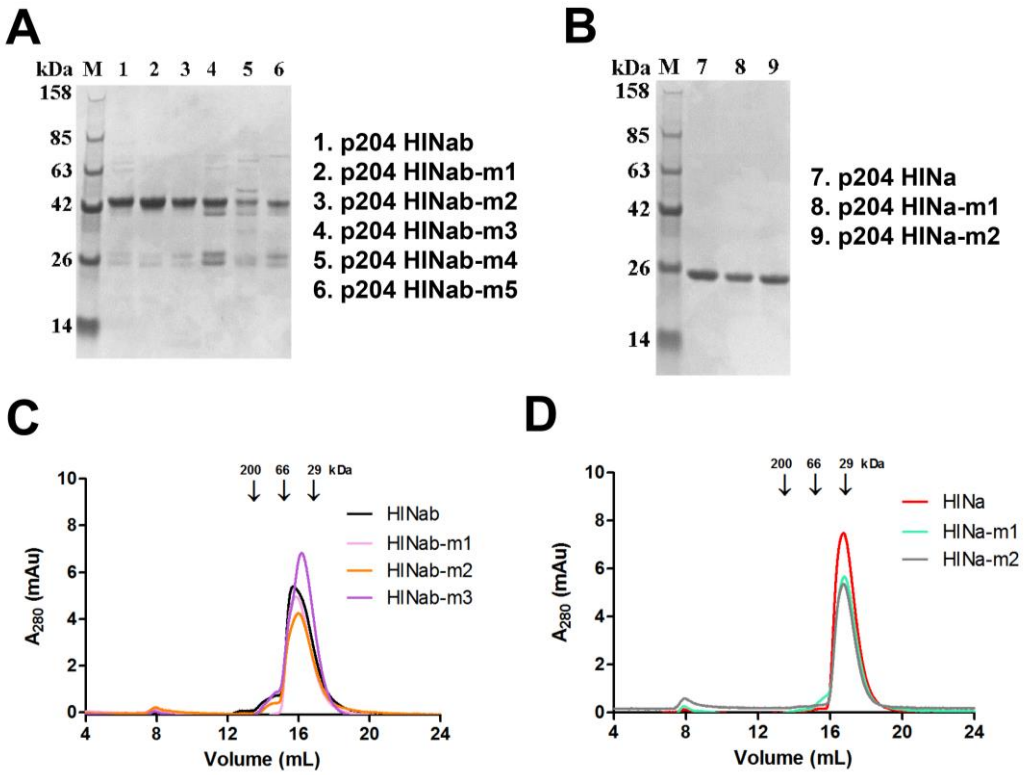

Figure S6. The purity and aggregation state of mutant p204 HINab and HINa domains. (A) and (B) SDS-PAGE images of purified p204 HINab mutants m1–m5 and HINa mutants m1–m2. (C) and (D) Size exclusion chromatography of purified p204 HINab mutants m1–m5 and HINa mutants m1–m2. All elution volumes correspond to monomers according to the marker (Sigma-Aldrich).

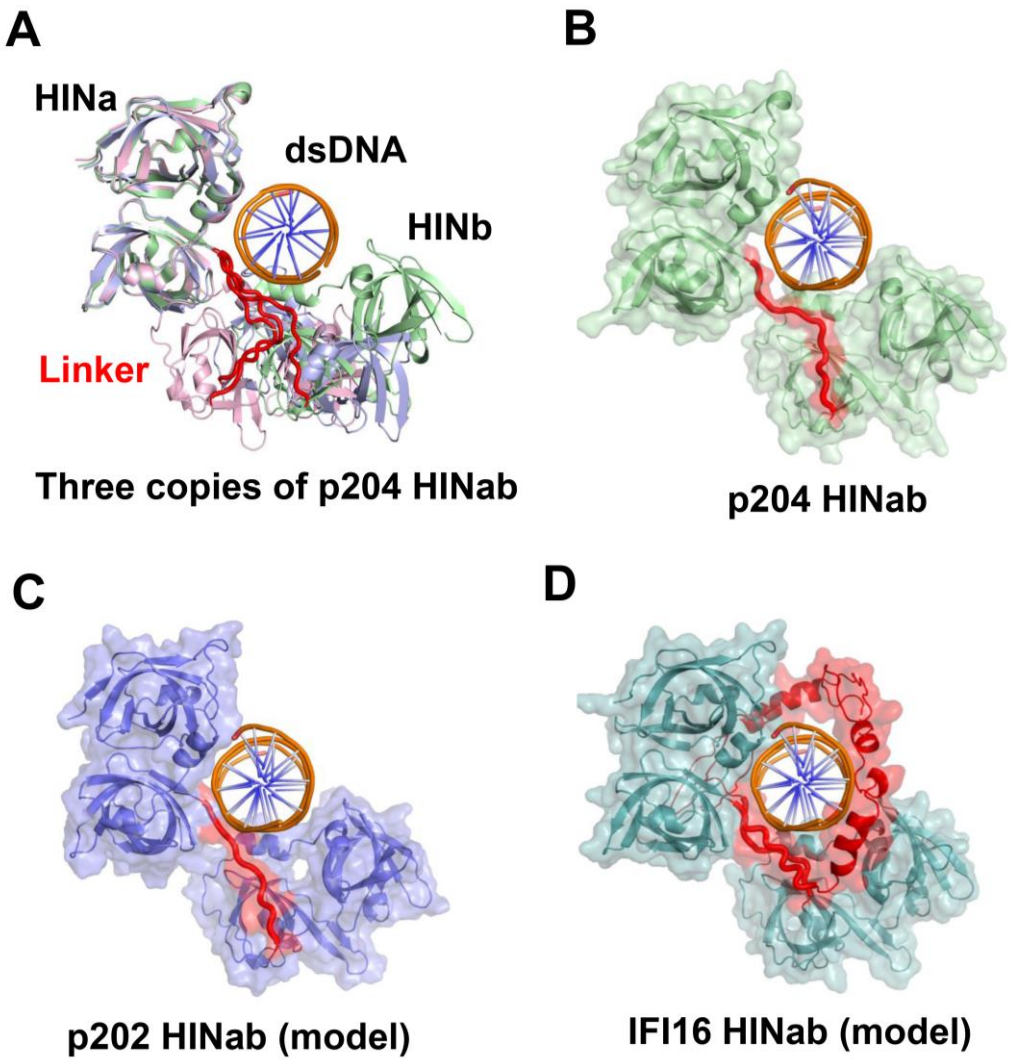

Figure S7. Different linker confirmations of HIN domains in p204, p202, and IFI16. (A) Linker confirmations of HIN domains in three copies of p204 HINab in complex with dsDNA. (B), (C), and (D) Linker confirmations of HIN domains in p204, p202, and IFI16. Linkers are shown in red. The linker of p202 and IFI16 HINab domain with dsDNA are modeled based on 5Z7D with 4L5R for p202, and 3RNU for IFI16. For clarification, one of two dsDNAs is omitted from the figures.

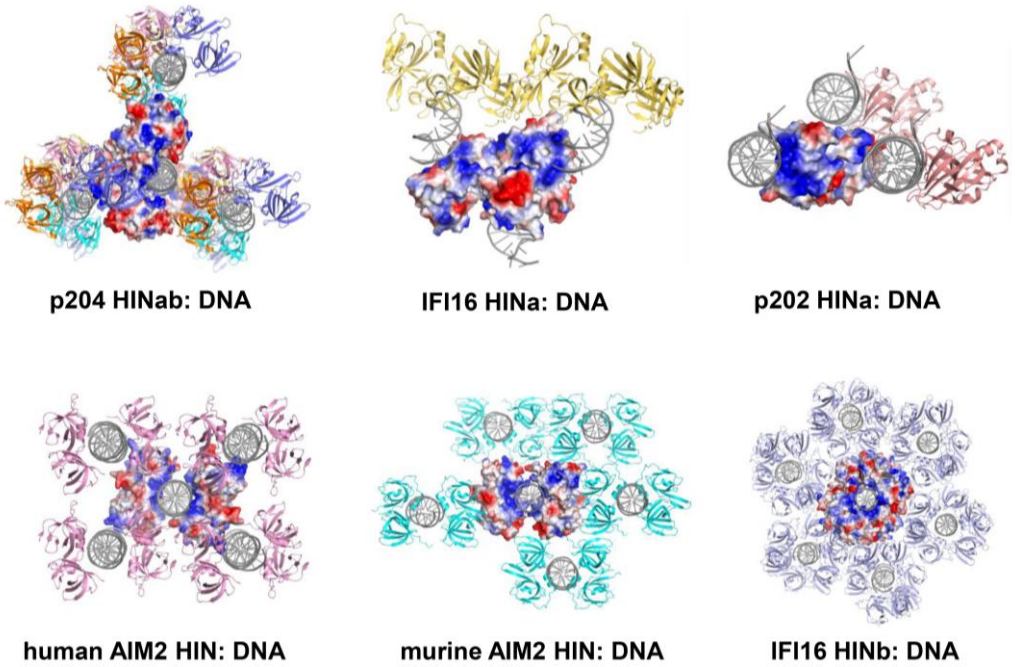

Figure S8. Structural analysis of HIN:DNA complexes in multiple asymmetry units. DNA is colored gray. HIN:DNA complex in one asymmetry unit are shown in surface electrostatics. The electrostatic potential is shown in blue (positive charges) and red (negative charges).